Quasi-two-dimensional *d*-spin and *p*-hole ordering in the three-dimensional perovskite $La_{1/3}Sr_{2/3}FeO_3$

J. Okamoto,[1,*] D. J. Huang,[1,2,†] K. S. Chao,[3] S. W. Huang,[3] C.-H. Hsu,[1] A. Fujimori,[4] A. Masuno,[5] T. Terashima,[6] M. Takano,[7] and C. T. Chen[1]

[1]*National Synchrotron Radiation Research Center, Hsinchu 30076, Taiwan*

[2]*Department of Physics, National Tsing Hua University, Hsinchu 30013, Taiwan*

[3]*Department of Electrophysics, National Chiao Tung University, Hsinchu 30010, Taiwan*

[4]*Department of Physics, Graduate School of Science, The University of Tokyo, Bunkyo-ku, Tokyo 113-0033, Japan*

[5]*Institute for Chemical Research, Kyoto University, Uji, Kyoto 611-0011, Japan*

[6]*Research Center for Low Temperature and Materials Science, Kyoto University, Uji, Kyoto 611-0011, Japan*

[7]*Institute for Integrated Cell-Material Sciences, Kyoto University, Sakyo-ku, Kyoto 606-8501, Japan*

(Received 18 August 2010; published 22 October 2010)

Measurements of resonant soft x-ray magnetic scattering reveal anomalous ordering of 3*d* spins and 2*p* holes in perovskite $La_{1/3}Sr_{2/3}FeO_3$, which is known to exhibit three-dimensional (3D) charge and spin ordering along the [111] direction. Upon cooling, a quasi-two-dimensional phase consisting of ferromagnetic and charge-disproportionated (111) trilayers of Fe^{3+}-Fe^{5+}-Fe^{3+} precedes the development of 3D magnetic ordering at the transition temperature, in sharp contrast to an ordinary transition from the paramagnetic and charge-uniform phase to the antiferromagnetic and charge-disproportionated phase expected according to conventional wisdom.

DOI: 10.1103/PhysRevB.82.132402 PACS number(s): 75.25.−j, 75.30.Ds, 75.30.Et, 78.70.Ck

The interplay among spin, charge and orbital degrees of freedom in transition-metal oxides couples transport to magnetism and yields many fascinating phenomena such as superconductivity, colossal magnetoresistance and magnetoelectric multiferroicity.[1–3] Many different phases and emergent properties of these materials are intimately connected with spin-charge ordering. Magnetite, which exhibits a phase transition known as the Verwey transition, shows a classic example of charge ordering.[4–6] There are also diverse manifestations of spin-charge ordering in other compounds. For instance, the charge-order transition of organic charge-transfer salts $(TMTTFT)_2X$ coincides with its onset of ferroelectric order;[7] charge ordering also takes place in the organic conductor $(DMe\text{-}DCNQI)_2Cu$.[8,9]

Fe-based perovskite is a system showing experimental evidence for the existence of charge ordering;[10–15] charge disproportionation is also manifested in this perovskite, for which two charge states of Fe ion were detected with Mössbauer spectroscopy.[10] Neutron diffraction has revealed a spin-density wave of sixfold periodicity along the [111] direction with a charge-density wave of threefold periodicity along the same direction.[13] Because of the charge disproportionation,[16,17] the magnetic structure of $La_{1/3}Sr_{2/3}FeO_3$ can be viewed as a stacking of ferromagnetic layers in a sequence nominally Fe^{3+}, Fe^{3+}, and Fe^{5+} along the [111] direction with strong interlayer magnetic interaction, as illustrated in Fig. 1(a), although the lattice structure is three-dimensionally (3D) isotropic. The spin coupling between Fe^{3+} and Fe^{5+} layers is ferromagnetic and much stronger than the antiferromagnetic coupling between two consecutive Fe^{3+} layers[17,18] because of the presence of holes on the oxygen orbitals arising from charge transfer from oxygen to the central "Fe^{5+}" of ferromagnetically coupled Fe^{3+}-Fe^{5+}-Fe^{3+} trilayers. This compound is hence an ideal system for studying the magnetic transition of layered oxides in the limit of strong interlayer coupling.

Here we report measurements of magnetic transitions of $La_{1/3}Sr_{2/3}FeO_3(111)$ thin films through hard and soft x-ray scattering on beamlines 13A1 and EPU at National Synchrotron Radiation Research Center (NSRRC) in Taiwan. Temperature-dependent measurements reveal that $La_{1/3}Sr_{2/3}FeO_3$ exhibits an anomalous two-step transition of spin-charge ordering associated with anisotropic properties. We discuss the phase transition associated with the quasi-two-dimensional (2D) *d*-spin and *p*-hole ordering in the 3D Fe perovskite.

Epitaxial $La_{1/3}Sr_{2/3}FeO_3(111)$ thin films of thickness 1000 Å were grown on $SrTiO_3(111)$ substrates by means of pulsed laser deposition. After deposition, the thin films were annealed for 80 min at 700 K under oxygen pressure 500 torr, and further capped with a protection layer (thickness 125 Å) of $SrTiO_3$. Using the four-probe method, we measured the electric resistivity and observed an anomaly about 195 K as shown in Fig. 1(b). Results of x-ray diffraction with energy 12.099 keV disclose the crystalline quality of the thin films and the existence of charge ordering. Figure 1(c) plots the scattering intensity as a scan of momentum transfer $\vec{q}$ along the [111] direction, i.e., a q_{111} scan, at 80 K. Fringes observed about the $SrTiO_3$ (1,1,1) reflection are the thickness fringes associated with the $SrTiO_3$ capping layer. Scattering signals with $\vec{q}=(\frac{2}{3},\frac{2}{3},\frac{2}{3})$ and $(\frac{4}{3},\frac{4}{3},\frac{4}{3})$ in reciprocal lattice units shown in Fig. 1(d) appear only for temperatures below 195 K, corresponding to the charge ordering originating from charge disproportionation. No magnetic ordering signal was observed at $\vec{q}=(\frac{1}{6},\frac{1}{6},\frac{1}{6})$ as the cross section of magnetic scattering was greatly diminished, when compared with that of charge scattering.[19]

With resonant soft x-ray magnetic scattering, we measured also the magnetic ordering of the $La_{1/3}Sr_{2/3}FeO_3$ thin film at $\vec{q}=(\frac{1}{6},\frac{1}{6},\frac{1}{6})$, which is concurrent with the charge ordering. The scattering plane was defined with vectors (1,1,1)

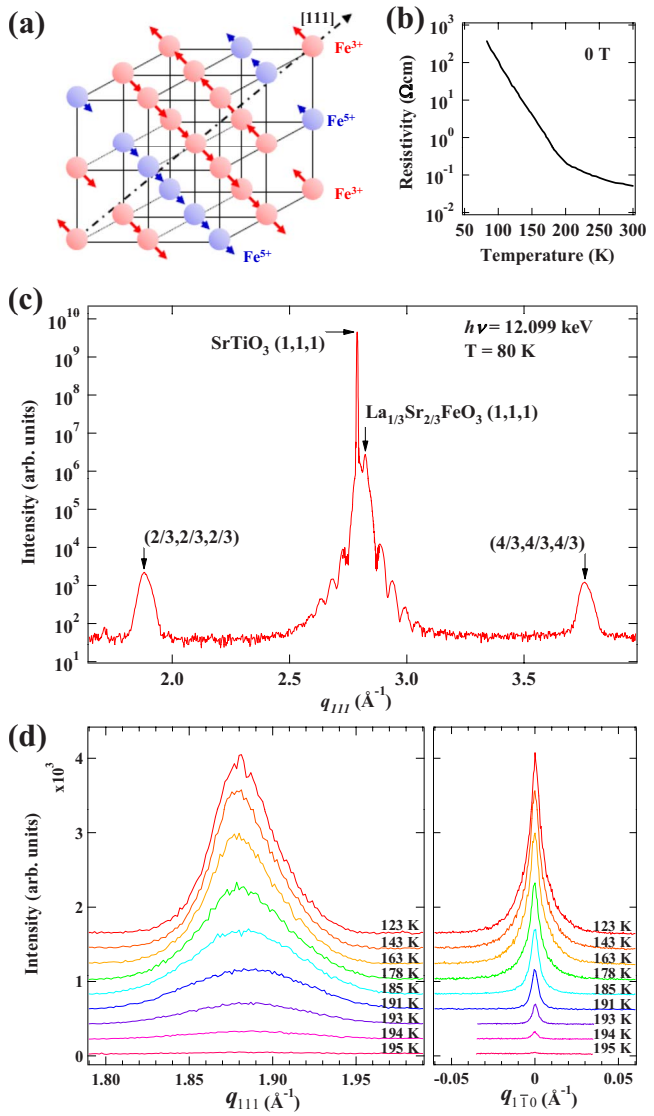

FIG. 1. (Color online) (a) Illustration of layered charge and magnetic structure of $La_{1/3}Sr_{2/3}FeO_3$ with charge disproportionation. (b) Temperature dependence of electric resistivity of $La_{1/3}Sr_{2/3}FeO_3(111)$. (c) Radial scan of x-ray scattering along [111] with an energy 12.099 keV measured at 80 K. (d) q scans of charge scattering along [111] and $[1\bar{1}0]$ with scattering vector $\vec{q}$ around $(\frac{2}{3},\frac{2}{3},\frac{2}{3})$ measured at various temperatures. All scans are offset vertically for clarity.

and $(1,\bar{1},0)$. The photon energy was tuned about the L_3 absorption edge of Fe, i.e., the $2p_{3/2} \rightarrow 3d$ transition. The **E** vector of the incident soft x-rays was set to be parallel to the scattering plane, i.e., π polarization. The experimental resolution of $\vec{q}$ along [111] in terms of half width at half maximum (HWHM) is estimated to be 0.001 $Å^{-1}$.

Scattering results, especially in a $q_{1\bar{1}0}$ scan, show a two-step transition in magnetic ordering. First, upon cooling from the paramagnetic phase, the magnetic ordering onsets at 195 K; scattering signals of magnetic ordering were observed in both q_{111} and $q_{1\bar{1}0}$ scans shown in Fig. 2(a), consistent with previous observations in bulk and thin-film $La_{1/3}Sr_{2/3}FeO_3$.[20–23] The scattering intensities of both q_{111}

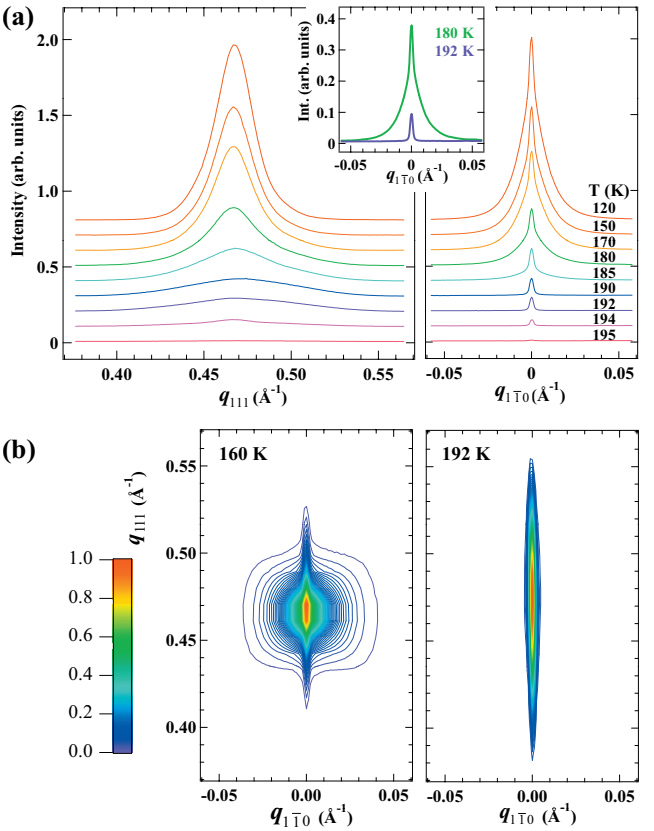

FIG. 2. (Color) Magnetic scattering of $La_{1/3}Sr_{2/3}FeO_3$ with $\vec{q} = (\frac{1}{6},\frac{1}{6},\frac{1}{6})$ measured with 707-eV soft x-rays at various temperatures. (a) Scans plotted against $\vec{q}$ along [111] and $[1\bar{1}0]$. All data are offset vertically for clarity. The inset compares $q_{1\bar{1}0}$ scans at 180 and 192 K. (b) Contour plots of magnetic scattering normalized to maximum intensity in the plane defined by q_{111} and $q_{1\bar{1}0}$ recorded at 160 and 192 K.

and $q_{1\bar{1}0}$ scans increased with decreasing temperature but the lineshape of their temperature dependence differed much. Upon cooling across 188 K, the lineshape of the q_{111} scan narrows gradually, and a new broad component in the $q_{1\bar{1}0}$ scan emerges abruptly. The inset of Fig. 2(a) highlights a comparison of lineshapes of the $q_{1\bar{1}0}$ scan at 180 K and 192 K. The reciprocal-space mapping of magnetic scattering in the scattering plane also unraveled the anisotropic properties of magnetic ordering, as displayed in Fig. 2(b). For temperatures between 188 and 195 K, the scattering distribution spreads mostly along the [111] direction, indicating anisotropic magnetic domains; the correlation length of interlayer magnetic ordering along [111] is much smaller than that of intralayer ordering. In contrast, the scattering image for temperatures below 188 K is less anisotropic, and, as explained below, such magnetic scattering comprised two components—3D short-range and quasi-2D long-range orderings.

We compare q_{111} and $q_{1\bar{1}0}$ scans of lattice, charge, and magnetic ordering at 160 and 192 K in Fig. 3. For charge and magnetic ordering, the lineshape of the q_{111} scan at 160 K is narrower than that at 192 K but the reverse for the $q_{1\bar{1}0}$ scan. In contrast, both q_{111} and $q_{1\bar{1}0}$ scans of the (111) Bragg reflections at 160 K are, respectively, identical to those at 192

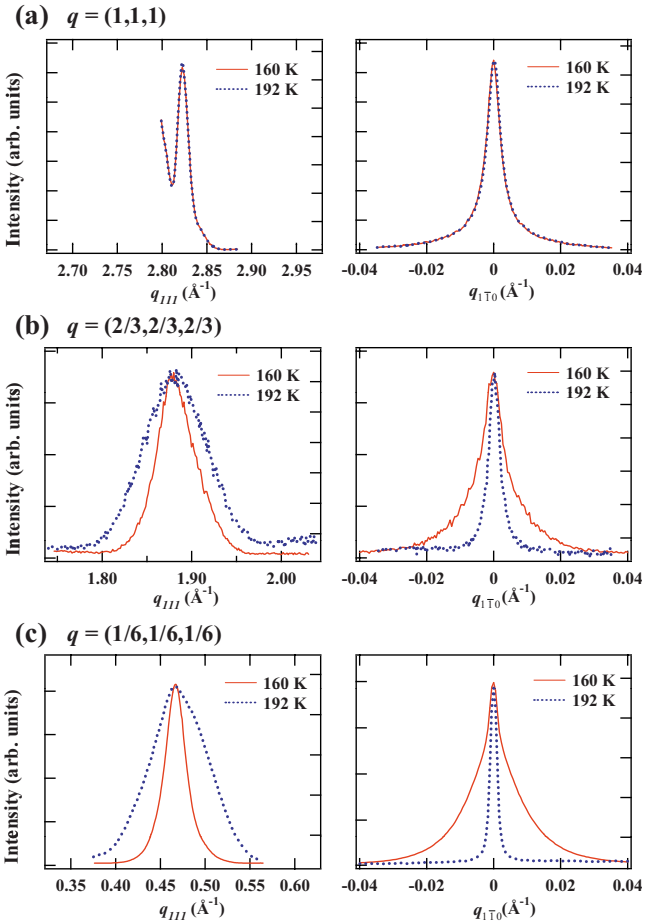

FIG. 3. (Color online) Comparison of q_{111} and $q_{1\bar{1}0}$ scans of x-ray scattering from lattice, charge and magnetic ordering in $La_{1/3}Sr_{2/3}FeO_3$ at 160 K and 192 K. The lattice signal with $\vec{q}=(1,1,1)$ (top panel), charge ordering with $\vec{q}=(\frac{2}{3},\frac{2}{3},\frac{2}{3})$ (middle panel), and magnetic ordering with $\vec{q}=(\frac{1}{6},\frac{1}{6},\frac{1}{6})$ (bottom panel) are scanned along q_{111} and $q_{1\bar{1}0}$. All spectra are normalized to maximum intensity.

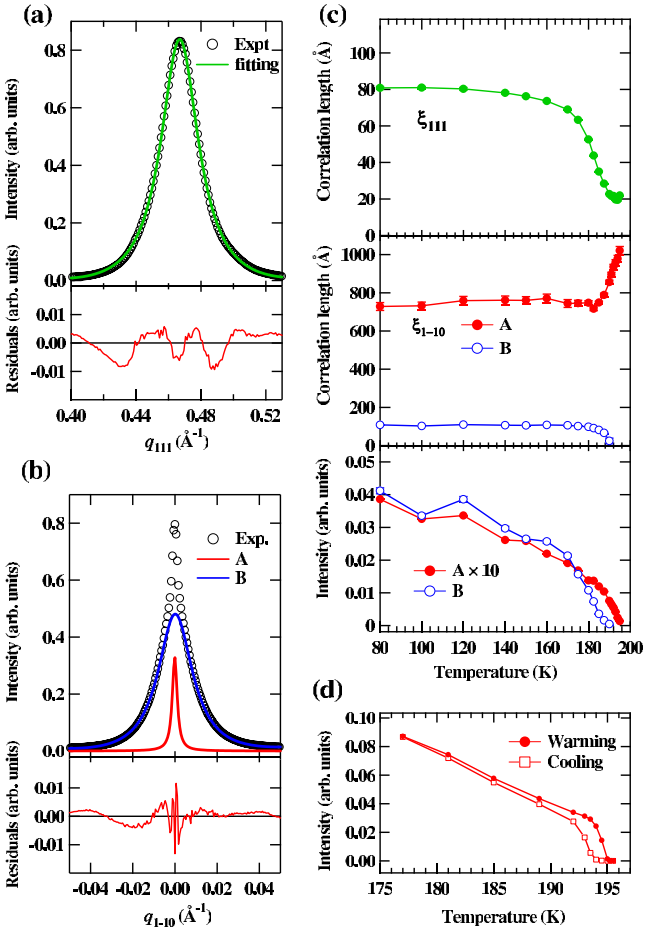

FIG. 4. (Color online) (a) and (b) q_{111} and $q_{1\bar{1}0}$ scans of magnetic scattering around $(\frac{1}{6},\frac{1}{6},\frac{1}{6})$ from $La_{1/3}Sr_{2/3}FeO_3$ at 160 K. The $q_{1\bar{1}0}$ scan is fit with two components for domains A and B. The chi squares (χ^2) of fit for q_{111} and $q_{1\bar{1}0}$ scans are 0.00347 and 0.00137, respectively. χ^2 is a weighted sum of squared errors defined by $\chi^2=\Sigma[(\text{data-fit})^2/\text{data}]$. (c) Temperature dependence of ξ_{111} and $\xi_{1\bar{1}0}$, and integrated intensities along $q_{1\bar{1}0}$. Open and closed circles correspond to domains A and B, respectively. (d) Thermal hysteresis of magnetic scattering from domain A.

K, indicating no structural transition concurrent with the magnetic transition. The magnetic and charge superstructure peaks have nearly the same temperature dependence, consistent with theoretical calculations[16] and neutron scattering results[17] which show that charge ordering in the charge disproportion is stabilized by the magnetic interaction.

There exist two steps in the observed magnetic transition. Between 188 and 195 K, there is one component in the lineshape of $q_{1\bar{1}0}$ scan. Below 188 K, there appears to exist two components in the lineshape of the $q_{1\bar{1}0}$ scan, which was fitted with two Lorentzian components denoted as A and B whereas the q_{111} lineshape is fitted with one component. The goodness of fit plotted in Figs. 4(a) and 4(b) indicates the fitting results are satisfactorily good. With the correlation length ξ defined as 1/HWHM, Fig. 4(c) compares the temperature dependence of correlation lengths along [111] and $[1\bar{1}0]$, i.e., ξ_{111} & $\xi_{1\bar{1}0}$, and the integrated intensities. As the scattering intensity from domain B for temperatures below 180 K is one order of magnitude larger than that of domain A, ξ_{111} below 180 K is determined mainly by domain B. In addition, domain A is anisotropic; $\xi^A_{1\bar{1}0}$ is much larger than ξ_{111} at all temperatures. From 195 to 188 K, $\xi^A_{1\bar{1}0}$ decreases from ~1000 to ~750 Å but ξ_{111} is nearly constant, ~20 Å. As temperature further decreases across 188 K, ξ_{111} gradually increases and attains a maximum ~80 Å whereas $\xi^A_{1\bar{1}0}$ remains ~750 Å. In contrast, domain B appears only at temperatures below 188 K and is almost isotropic. The scattering intensities of both domains increase with decreasing temperature but domain B with $\xi^B_{1\bar{1}0}\sim 100$ Å dominates the magnetic ordering at low temperatures.

The transition at 195 K is a first-order transition because there exists a thermal hysteresis, as shown in Fig. 4(d). Based on the exchange interaction between two neighboring Fe layers through the intervening O layer,[17,18] we propose the following scenario for understanding this magnetic transition involved with a paramagnetic charge-uniform state and an antiferromagnetic

charge-disproportionated state. In $La_{1/3}Sr_{2/3}FeO_3$, the strongly coupled ferromagnetic Fe^{3+}-Fe^{5+}-Fe^{3+} trilayer[24] is stabilized by oxygen holes adjacent to the central Fe^{5+} layer to form a 2D quasilong-range magnetically ordered object. The ground state of the nominal Fe^{5+} is actually dominated by $d^5\underline{L}^2$, where $\underline{L}$ denotes a hole in the oxygen $2p$ band.[18] In other words, the $2p$ holes are concentrated and confined in two thirds of the oxygen layers, playing a crucial role in the complicated magnetism. The $2p$ holes concentrate homogeneously in the charge-uniform state whereas double hole-concentrated O layers and a single-hole O layer stack alternatively in the charge-disproportionated state. In the early stage of transition from high temperature, trilayers which antiferromagnetically stack along the [111] direction nucleate and grow independently; these trilayers are not necessarily in phase and thus the 3D ordering is partially frustrated, as evidenced by the large width of the corresponding charge and magnetic scattering. In addition, the precipitation of the trilayers is further stabilized by the lattice. As $La_{1/3}Sr_{2/3}FeO_3$ is a rhombohedrally distorted perovskite, the rhombohedral distortion stabilizes the $(1,1,1)$ orientation over the other orientations $(1,1,-1)$, $(1,-1,1)$, and $(-1,1,1)$.

In conclusion, we have unraveled that quasi-2D ordering of $3d$ spins and $2p$ holes indeed exists in perovskite $La_{1/3}Sr_{2/3}FeO_3$ which has a 3D lattice structure. This classic material exhibits a unique transition of spin-charge ordering which involves a crossover of dimensionality. Upon cooling, the formation of the ferromagnetic and charge-disproportionated trilayers precedes the development of 3D magnetic order.

We thank NSRRC staff, particularly W. B. Wu, C. S. Lee, and H. W. Fu for their technical support. We are grateful to H. Wadati and H. Nakao for discussions. This work was supported by the National Science Council of Taiwan, and a Grant-in-Aid for Scientific Research (Grant No. S17105002) from JSPS, Japan.

*Present address: Photon Factory, Institute of Materials Structure Science, High Energy Accelerator Research Organization, 1-1 Oho, Tsukuba, Ibaraki 305-0801 Japan.

†Corresponding author; djhuang@nsrrc.org.tw

[1] M. Imada, A. Fujimori, and Y. Tokura, Rev. Mod. Phys. **70**, 1039 (1998).

[2] Y. Tokura and N. Nagaosa, Science **288**, 462 (2000).

[3] S.-W. Cheong and M. V. Mostovoy, Nature Mater. **6**, 13 (2007).

[4] E. J. W. Verwey, Nature (London) **144**, 327 (1939) London.

[5] A. Zabet-Khosousi, P. E. Trudeau, Y. Suganuma, A. A. Dhirani, and B. Statt, Phys. Rev. Lett. **96**, 156403 (2006).

[6] D. J. Huang, H.-J. Lin, J. Okamoto, K. S. Chao, H.-T. Jeng, G. Y. Guo, C.-H. Hsu, C.-M. Huang, D. C. Ling, W. B. Wu, C. S. Yang, and C. T. Chen, Phys. Rev. Lett. **96**, 096401 (2006).

[7] M. de Souza, P. Foury-Leylekian, A. Moradpour, J.-P. Pouget, and M. Lang, Phys. Rev. Lett. **101**, 216403 (2008).

[8] I. H. Inoue, A. Kakizaki, H. Namatame, A. Fujimori, A. Kobayashi, R. Kato, and H. Kobayashi, Phys. Rev. B **45**, 5828 (1992).

[9] Y. Shinohara, S. Kazama, K. Mizoguchi, M. Hiraoka, and H. Sakamoto, Shin-ichi Masubuchi, R. Kato, K. Hiraki, and T. Takahashi, Phys. Rev. B **76**, 035128 (2007).

[10] M. Takano, N. Nakanishi, Y. Takeda, S. Naka, and T. Takada, Mater. Res. Bull. **12**, 923 (1977).

[11] P. M. Woodward, D. E. Cox, E. Moshopoulou, A. W. Sleight, and S. Morimoto, Phys. Rev. B **62**, 844 (2000).

[12] M. Takano, J. Kawachi, N. Nakanishi, and Y. Takeda, J. Solid State Chem. **39**, 75 (1981).

[13] P. D. Battle, T. C. Gibb, and P. Lightfoot, J. Solid State Chem. **84**, 271 (1990).

[14] J. Blasco, B. Aznar, J. Garcia, G. Subias, J. Herrero-Martin, and J. Stankiewicz, Phys. Rev. B **77**, 054107 (2008).

[15] J. Herrero-Martin, G. Subias, J. Garcia, J. Blasco, and M. Concepcion Sanchez, Phys. Rev. B **79**, 045121 (2009).

[16] T. Mizokawa and A. Fujimori, Phys. Rev. Lett. **80**, 1320 (1998).

[17] R. J. McQueeney, J. Ma, S. Chang, J.-Q. Yan, M. Hehlen, and F. Trouw, Phys. Rev. Lett. **98**, 126402 (2007).

[18] J. Matsuno, T. Mizokawa, A. Fujimori, K. Mamiya, Y. Takeda, S. Kawasaki, and M. Takano, Phys. Rev. B **60**, 4605 (1999).

[19] M. Blume, J. Appl. Phys. **57**, 3615 (1985).

[20] T. Ishikawa, S. K. Park, T. Katsufuji, T. Arima, and Y. Tokura, Phys. Rev. B **58**, R13326 (1998).

[21] S. K. Park, T. Ishikawa, Y. Tokura, J. Q. Li, and Y. Matsui, Phys. Rev. B **60**, 10788 (1999).

[22] H. Wadati, D. Kobayashi, H. Kumigashira, K. Okazaki, T. Mizokawa, A. Fujimori, K. Horiba, M. Oshima, N. Hamada, M. Lippmaa, M. Kawasaki, and H. Koinuma, Phys. Rev. B **71**, 035108 (2005).

[23] K. Ueno, A. Ohtomo, F. Sato, and M. Kawasaki, Phys. Rev. B **73**, 165103 (2006).

[24] For clarity, a trilayer of Fe^{3+}-O-Fe^{5+}-O-Fe^{3+} is denoted Fe^{3+}-Fe^{5+}-Fe^{3+}.